Development 135, 3989-3993 (2008) doi:10.1242/dev.029736

Attribution of vascular phenotypes of the murine *Egfl7* locus to the microRNA *miR-126*

Frank Kuhnert[1,*], Michael R. Mancuso[1,*], Jessica Hampton[1], Kryn Stankunas[2], Tomoichiro Asano[3], Chang-Zheng Chen[4] and Calvin J. Kuo[1,†]

Intronic microRNAs have been proposed to complicate the design and interpretation of mouse knockout studies. The endothelial-expressed *Egfl7*/*miR-126* locus contains *miR-126* within *Egfl7* intron 7, and angiogenesis deficits have been previously ascribed to *Egfl7* gene-trap and *lacZ* knock-in mice. Surprisingly, selectively floxed $Egfl7^{\Delta}$ and $miR\text{-}126^{\Delta}$ alleles revealed that $Egfl7^{\Delta/\Delta}$ mice were phenotypically normal, whereas $miR\text{-}126^{\Delta/\Delta}$ mice bearing a 289-nt microdeletion recapitulated previously described *Egfl7* embryonic and postnatal retinal vascular phenotypes. Regulation of angiogenesis by *miR-126* was confirmed by endothelial-specific deletion and in the adult cornea micropocket assay. Furthermore, *miR-126* deletion inhibited VEGF-dependent Akt and Erk signaling by derepression of the p85β subunit of PI3 kinase and of Spred1, respectively. These studies demonstrate the regulation of angiogenesis by an endothelial miRNA, attribute previously described *Egfl7* vascular phenotypes to *miR-126*, and document inadvertent miRNA dysregulation as a complication of mouse knockout strategies.

KEY WORDS: Angiogenesis, miRNA, *miR-126* (*Mirn126*), Egfl7, p85β (Pik3r2)

INTRODUCTION

MicroRNAs (miRNAs) are essential regulators of physiology and pathophysiology (Zhao and Srivastava, 2007). The inadvertent dysregulation of intronic miRNAs has been predicted to be a general complication in the design and interpretation of mouse knockout studies (Osokine et al., 2008). *miR-126* (*Mirn126* – Mouse Genome Informatics) is an endothelial miRNA residing within intron 7 of *Egfl7*, resulting in pan-vascular developmental coexpression of *miR-126* and *Egfl7* and their abundant expression in cultured endothelium (Fitch et al., 2004; Kloosterman et al., 2006; Kuehbacher et al., 2007; Poliseno et al., 2006). *Egfl7* is an endothelial secreted extracellular matrix protein, which, in zebrafish, regulates embryonic vascular tube assembly (De Maziere et al., 2008; Parker et al., 2004). In vitro, various functions have been ascribed to *Egfl7*, including the regulation of endothelial or vascular smooth muscle migration and adhesion (Campagnolo et al., 2005; Parker et al., 2004; Soncin et al., 2003). Two different mouse knockout alleles of *Egfl7* have been described: a gene-trap insertion into intron 2, and an IRES *lacZ* knock-in replacing exons 5-7, both upstream of *miR-126* in intron 7. Both the *Egfl7* gene-trap and *lacZ* knock-in are associated with edema, angiogenic deficits and ~50% embryonic lethality (Schmidt et al., 2007). Here, we explored the functions of both *Egfl7* and its embedded miRNA, *miR-126*, using floxed alleles to selectively disrupt each gene without reciprocal perturbation.

[1]Division of Hematology and [2]Division of Cardiovascular Medicine, Department of Medicine, Stanford University School of Medicine, CCSR 1155, 269 Campus Drive, Stanford, CA 94305, USA. [3]Department of Medical Science, Graduate School of Medicine, University of Hiroshima, 1-2-3 Kasumi, Minami-ku, Hiroshima City, Hiroshima 734-8553, Japan. [4]Baxter Laboratory and Department of Microbiology and Immunology, Stanford University School of Medicine, Stanford, CA 94305, USA.

*These authors contributed equally to this work
†Author for correspondence (e-mail: cjkuo@stanford.edu)

Accepted 7 October 2008

MATERIALS AND METHODS

Generation of $Egfl7^{\Delta/\Delta}$ and $miR\text{-}126^{\Delta/\Delta}$ mice

For targeting *Egfl7*, a loxP site (Pl452) and a neomycin selection cassette plus a loxP site (Pl451) were cloned into an *Afl*II site 5′ of exon 5 and into an *Nhe*I site 3′ of exon 7, respectively. For targeting the 73-bp *miR-126* precursor, Pl452 and Pl451 were cloned into an *Nhe*I site 194 bp 5′ of *miR-126* and an *Nsi*I site 22 bp 3′ of *miR-126*, respectively (flanking 289 bp total) (for details, see Figs S1 and S2 in the supplementary material). Delta (Δ) alleles were generated by crossing to *CMV-* or *HPRT-Cre* mice. Mutant mice were analyzed in a mixed 129sV/C57Bl/6 genetic background. All mice were treated according to the Stanford Institutional Animal Care and Use Committee and the Stanford Administrative Panel on Laboratory Animal Care.

miRNA in situ hybridization

In situ hybridization was performed as described (Obernosterer et al., 2007). Mouse *miR-126* locked nucleic acid (LNA) probes were from Exiqon.

Generation of rabbit anti-Egfl7 antibody and immunofluorescence staining

Rabbits were immunized against the bacterially expressed C-terminal 112 amino acids of murine Egfl7 fused to the C-terminus of maltose binding protein (MBP). Antiserum was affinity purified against the C-terminal 112 amino acids of Egfl7 fused to the C-terminus of glutathione-S-transferase (GST). PFA-fixed frozen uterus sections were stained with 0.1 μg of affinity-purified rabbit anti-Egfl7 antibody and imaged with a Zeiss Z1 Axioimager with Apotome.

Quantitative real-time PCR

miR-126 expression was analyzed using the Taqman MicroRNA Assay (Applied Biosystems) utilizing looped RT primers to detect processed *miR-126*, and expression was normalized to that of *miR-16*. *Egfl7* expression was determined using the SYBR Green Quantitect PCR Kit (Qiagen) and normalized to that of *Gapdh*. *Egfl7* primers: 5′-TGCGACGGAC-ACAGAGCCTGCA-3′ and 5′-CAAGTATCTCCCTGCCATCCCA-3′. Assays were performed in triplicate and results from at least three independent experiments are presented.

Whole-mount retina staining

P5 eyes were dissected and fixed in 4% paraformaldehyde (PFA) in PBS overnight at 4°C. Retinas were isolated, blocked in PBS containing 1% BSA and 0.5% Triton X-100 overnight at 4°C, incubated overnight with 10 μg of FITC-conjugated isolectin B4 (Vector Labs) in 500 μl of the same solution, washed and then flat mounted.

Western blot analysis

Antibodies used were: rabbit anti-p85, rabbit anti-phospho-Akt (Akt1 – Mouse Genome Informatics) (Ser 473), rabbit anti-phospho-Erk (Mapk1 – Mouse Genome Informatics) (all from Cell Signaling), rabbit anti-Spred1, rabbit anti-p85β, rabbit anti-α-actin (all from Abcam) and rat anti-HA (Roche).

Transfection of human umbilical vein endothelial cells (HUVEC) with miRNA inhibitor

Anti-*miR-126* hairpin inhibitors (Thermo Scientific Dharmacon) or negative control inhibitor were transfected into HUVEC at 100 nM using Dharmafect1. Cells were assayed for protein expression 48 hours after transfection.

Scratch wound assay

HUVEC were serum starved overnight 24 hours after transfection of miRNA inhibitors, and scraped with a sterile P200 tip to generate a cell-free zone. Cells were stimulated with human $VEGF_{165}$ (R&D Systems) (10 ng/ml) for 24 hours. Migration was quantified by counting the number of cells per scratched area (n=6).

Corneal micropocket assay

The corneal micropocket assay was performed as described (Kuo et al., 2001).

miR-126 target luciferase reporter assay

The 3′UTR of *Pik3r2* and *Spred1* were amplified and cloned downstream of a *Renilla* luciferase reporter gene. The *miR-126* binding sites were mutated from 5′-ACGGTAC-3′ to 5′-GTAACGA-3′ and from 5′-GGTACG-3′ to 5′-AAGCAT-3′ in the 3′UTR of *Pik3r2* and *Spred1*, respectively. The *Lin41* (*Trim71* – Mouse Genome Informatics) 3′UTR was used as a negative control. 293T cells in 24-well plates were transfected with 3.35 ng/well of firefly luciferase, 0.667 ng/well of *Renilla* 3′UTR construct, and either 0, 10 or 100 ng/well of *miR-126* expression vector. Empty vector was added to provide a total of 337 ng of DNA per transfection. Forty-eight hours after transfection, the *Renilla*/firefly luciferase was measured using the Dual Reporter Luciferase Kit (Promega).

Akt/Erk phosphorylation assay

Akt/Erk phosphorylation assays were performed as described (Gerber et al., 1998).

Statistical analysis

P-values were determined using a two-tailed Student's *t*-test assuming unequal variances.

RESULTS AND DISCUSSION

We explored the mouse *Egfl7/miR-126* locus using selectively floxed $Egfl7^{\Delta}$ and $miR\text{-}126^{\Delta}$ alleles to replace either a 289 bp segment of intron 7 containing *miR-126* or exons 5-7 of *Egfl7* with a single loxP site, without disruption of the reciprocal gene or miRNA (Fig. 1A; see Figs S1 and S2 in the supplementary material). $miR\text{-}126^{\Delta/\Delta}$, but not $Egfl7^{\Delta/\Delta}$, embryos exhibited loss of *miR-126* expression as assessed by in situ hybridization or quantitative PCR (qPCR) using looped RT primers to detect processed *miR-126* (Fig. 1B,C). Conversely, $Egfl7^{\Delta/\Delta}$, but not $miR\text{-}126^{\Delta/\Delta}$, mice exhibited loss of *Egfl7* by qPCR and by immunofluorescence with an affinity-purified rabbit anti-Egfl7 antiserum (Fig. 1C,D). Furthermore, sequencing of the *Egfl7* ORF amplified from $miR\text{-}126^{\Delta/\Delta}$ cDNA revealed a lack of occult *Egfl7* splicing alterations resulting from the *miR-126* microdeletion (Fig. 1E). These studies indicated the successful generation of two monospecific *Δ* alleles for *miR-126* and *Egfl7*, respectively.

Surprisingly, $Egfl7^{\Delta/\Delta}$ mice were phenotypically normal and born at the expected Mendelian ratios despite previous reports from gene-trap and conventional knockout alleles (Schmidt et al., 2007) (Fig. 2A). By contrast, $miR\text{-}126^{\Delta/\Delta}$ mice recapitulated numerous previously described *Egfl7* mutant phenotypes (Schmidt et al., 2007)

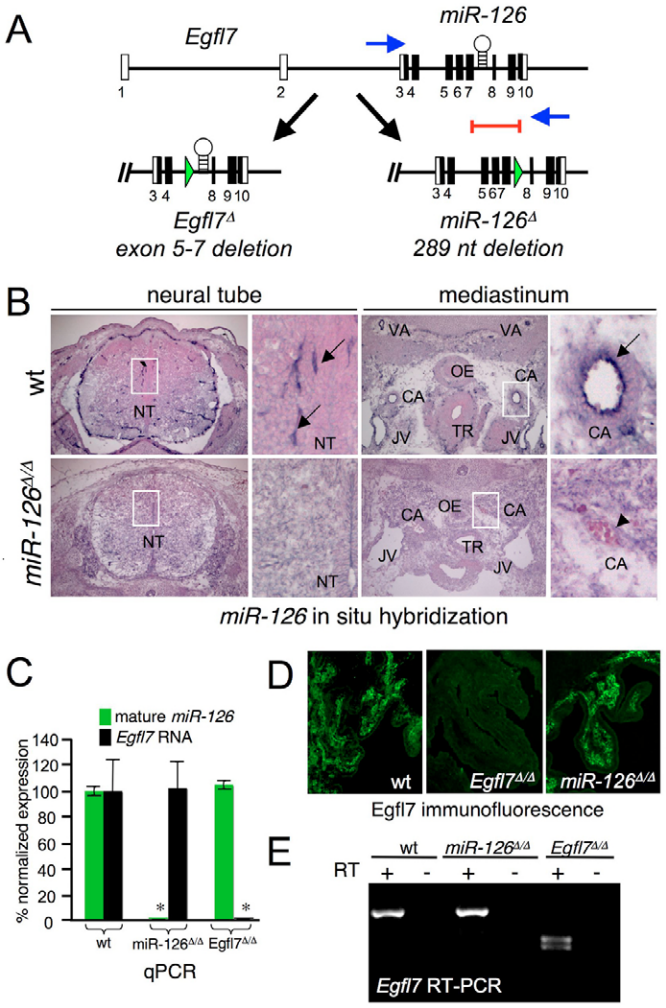

Fig. 1. Generation and validation of *Egfl7* and *miR-126* deletion alleles. (**A**) *Egfl7* and *miR-126* delta (Δ) alleles were generated by flanking exons 5-7 of *Egfl7* or a 289 bp segment of intron 7 containing *miR-126* with loxP sites, respectively, followed by in vivo deletion using Cre recombinase. Green arrowheads, remnant loxP sites after Cre deletion. Blue arrows, PCR primers used in E. Red line, Egfl7 epitope used for polyclonal antibody generation. (**B**) In situ hybridization for processed *miR-126* (dark purple staining) demonstrates vascular expression in the trunk region of wild-type (wt) E14.5 mouse embryos (top panels) that is absent in $miR\text{-}126^{\Delta/\Delta}$ embryos (bottom panels). Arrows in higher magnification images (taken from the boxed regions) highlight vascular *miR-126* expression in the neural tube and carotid artery in wild-type embryos, and arrowheads the absence thereof in $miR\text{-}126^{\Delta/\Delta}$ embryos. CA, carotid artery; JV, jugular vein; NT, neural tube; OE, esophagus; TR, trachea; VA, vertebral artery. (**C**) Quantitative PCR (n=6) confirmed the absence of *Egfl7* mRNA in $Egfl7^{\Delta/\Delta}$ embryos and the absence of mature (processed) *miR-126* in $miR\text{-}126^{\Delta/\Delta}$ embryos. A looped RT primer specifically detecting the mature *miR-126* processed end was utilized. Notably, $Egfl7^{\Delta/\Delta}$ embryos exhibited normal *miR-126* processing and $miR\text{-}126^{\Delta/\Delta}$ embryos exhibited normal levels of *Egfl7* mRNA, indicating that microdeletion did not disrupt physiological expression of the adjacent gene/miRNA in either case. *P<0.001 versus wild type. (**D**) Immunofluorescence staining of uterus from a pregnant mouse with affinity-purified rabbit anti-Egfl7 antibody demonstrating loss of Egfl7 protein in adult $Egfl7^{\Delta/\Delta}$, but not adult $miR\text{-}126^{\Delta/\Delta}$, mice. (**E**) RT-PCR of full-length *Egfl7* coding sequence from $miR\text{-}126^{\Delta/\Delta}$ embryos indicates that microdeletion of *miR-126* does not induce occult splicing of *Egfl7* mRNA. A doublet is present in $Egfl7^{\Delta/\Delta}$ embryos representing out-of-frame splicing from exon 4 to exon 8 or 9.

A

Egfl7	+/+	+/Δ	Δ/Δ
E14.5	10	20	13(0)
P21	49	100	56

B

miR-126	+/+	+/Δ	Δ/Δ
E12.5	21	41	22(0)
E14.5	13	28	17(9)
P21	64	111	30

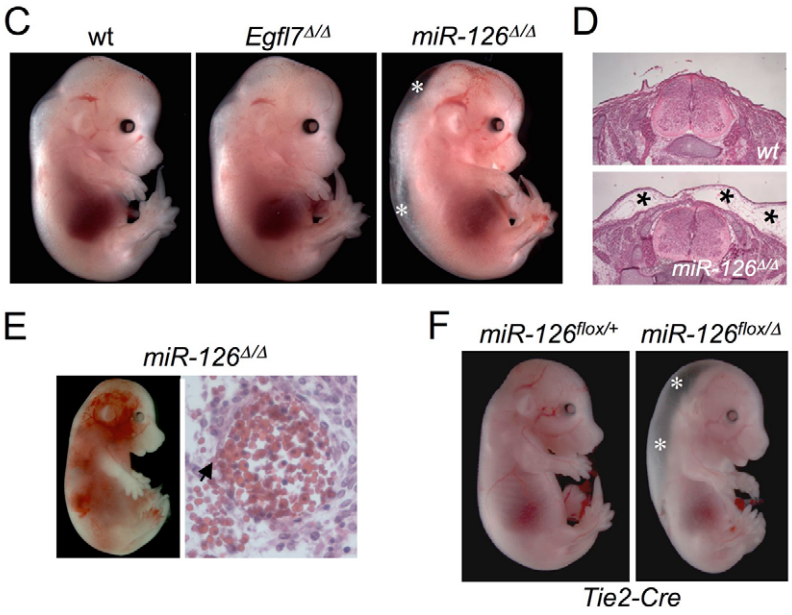

Fig. 2. *miR-126*$^{Δ/Δ}$, but not *Egfl7*$^{Δ/Δ}$, mice exhibit incompletely penetrant embryonic lethality, edema and vascular leakage. (**A**,**B**) Breeding tables from heterozygous intercrosses show that *Egfl7*$^{Δ/Δ}$ mice are born at normal Mendelian ratios (χ^2=0.741), whereas *miR-126*$^{Δ/Δ}$ embryos exhibit ~50% embryonic/perinatal lethality (χ^2<0.001). Numbers in parenthesis indicate embryos found with edema. Red numbers indicate deviation from Mendelian ratios. (**C**) Wild-type (wt) and *Egfl7*$^{Δ/Δ}$ embryos were phenotypically indistinguishable, whereas 50% of the *miR-126*$^{Δ/Δ}$ embryos displayed subcutaneous edema (*) at E14.5. (**D**) Hematoxylin and Eosin staining reveals the severity of the edema (*) in E14.5 embryos. (**E**) Varying degrees of subcutaneous hemorrhage are detected in ~20% of E15.5 *miR-126*$^{Δ/Δ}$ embryos; a severely affected embryo is depicted. Histological analysis shows red blood cells extravasating from a representative ruptured, leaky vessel (arrow). (**F**) Tie2-Cre-mediated endothelial deletion of *miR-126* phenocopies the *miR-126*$^{Δ/Δ}$ edema (*) phenotype.

including ~50% embryonic lethality (Fig. 2B), which appeared obligately associated with the development of prominent subcutaneous embryonic edema by E14.5 (Fig. 2C,D). At E15.5, multifocal, progressive hemorrhage of varying severity from ruptured blood vessels was observed in ~20% of the *miR-126*$^{Δ/Δ}$ embryos, most prominently in the jugular and subcutaneous regions (Fig. 2E), with resultant embryonic lethality becoming first apparent at E16.5. The embryonic edema was phenocopied by *miR-126*$^{flox//Δ}$*;Tie2-Cre* embryos, consistent with a cell-autonomous mechanism in the endothelium (Fig. 2F).

Surviving *miR-126*$^{Δ/Δ}$ neonates, which were obtained at ~50% of the expected frequency (Fig. 2B), exhibited delayed postnatal retinal angiogenesis (Fig. 3A-C). This was particularly notable in terms of compromised radial migration, a decreased area of retinal

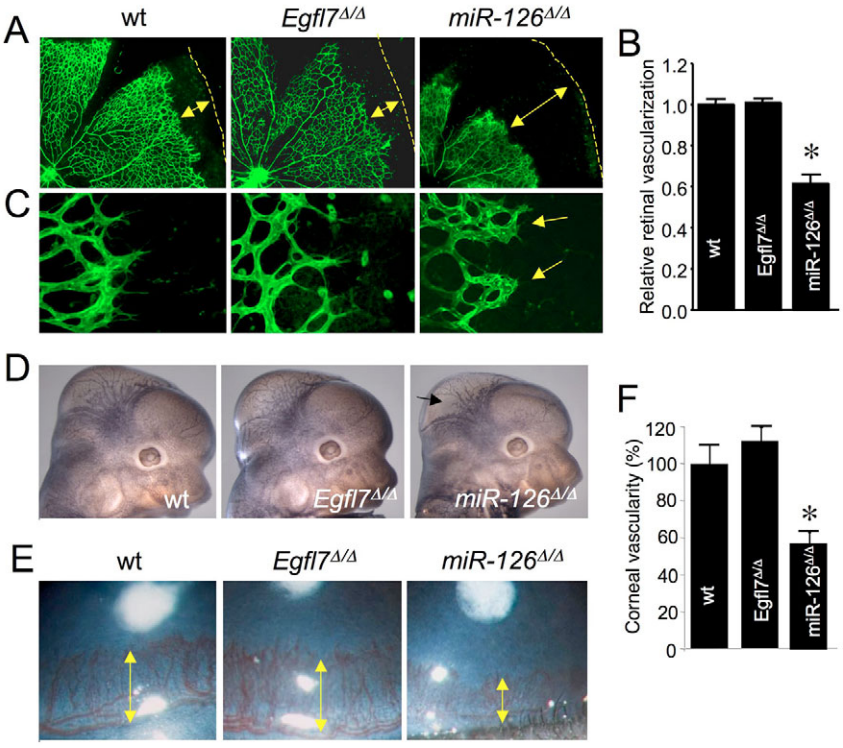

Fig. 3. Angiogenesis phenotypes in *miR-126*$^{Δ/Δ}$ embryos. (**A**) Isolectin B4 staining of P5 postnatal retinas. Retinal vascularization was normal in *Egfl7*$^{Δ/Δ}$ mice but was severely delayed in *miR-126*$^{Δ/Δ}$ mice as indicated by arrows. The dashed line indicates the edge of the optic cup. wt, wild type. (**B**) Quantitation of retinal vascularization demonstrates a ~40% reduction of retinal vascular coverage in *miR-126*$^{Δ/Δ}$ mice. (**C**) High-magnification images of retinal vascular sprouts. Note the marked thickening (arrows) of vascular sprouts in *miR-126*$^{Δ/Δ}$ retinas as compared with wild-type or *Egfl7*$^{Δ/Δ}$ mice. (**D**) CD31 (Pecam1) whole-mount staining of E12.5 heads. Note the delayed vascularization and reduced complexity (arrow) of the cranial vasculature in *miR-126*$^{Δ/Δ}$ embryos. (**E**) Adult animals of the indicated genotypes (*n*=7) received corneal implants of slow-release hydron pellets containing VEGF. Neovascularization was quantified after 6 days by slit lamp examination. Arrows highlight the length of vessel growth. (**F**) Adult *miR-126*$^{Δ/Δ}$ mice exhibited ~50% impairment of corneal vascularization relative to *Egfl7*$^{Δ/Δ}$ or wild-type mice.

vascularization, and abnormally thickened endothelial sprouts (Fig. 3A-C), as previously described in *Egfl7* gene-trap and knock-in mice (Schmidt et al., 2007). *miR-126*$^{\Delta/\Delta}$ mice further displayed delayed developmental cranial angiogenesis (Fig. 3D), again reminiscent of previously described *Egfl7* mutant phenotypes (Schmidt et al., 2007). Consistent with a more substantial role for *miR-126* in the regulation of adult angiogenic processes, surviving *miR-126*$^{\Delta/\Delta}$ mice demonstrated impaired angiogenesis in a VEGF-dependent corneal micropocket assay (Fig. 3E,F). None of the aforementioned phenotypes was observed in *Egfl7*$^{\Delta/\Delta}$ or wild-type mice (Fig. 3A-F), with the deficits in retinal, head and corneal vasculature all supporting the in vivo regulation of angiogenesis by *miR-126.*

The mechanisms of *miR-126* regulation of angiogenesis were further explored in cultured endothelial cells. Transfection of an RNA hairpin inhibitor induced a greater than 95% depletion of mature *miR-126* in HUVEC (Fig. 4A). This was accompanied by significant decreases in migration in scratch assays, as well as impaired VEGF-dependent activation of the downstream kinase Akt (Fig. 4B,C). The basis for this impaired VEGF signaling in *miR-126*-deficient endothelium was examined at the level of miRNA target genes. *miR-126* directly repressed expression of the *Pik3r2*-encoded p85β subunit of PI3 kinase (PI3K) in co-transfection assays, whereas p85β protein was increased in both primary *miR-126*$^{\Delta/\Delta}$ endothelium and *miR-126* knockdown HUVEC (Fig. 4D-G). Either the knockdown of *miR-126* or the overexpression of the target p85β in HUVEC was sufficient to impair VEGF-mediated activation of the PI3K downstream target Akt, paralleling inhibition of insulin receptor tyrosine kinase signaling by p85 overexpression (Barbour et al., 2005; Brachmann et al., 2005; Ueki et al., 2002) (Fig. 4C,H). *miR-126* knockdown additionally impaired VEGF activation of Erk (Fig. 4C), further reiterating compromised signal transduction in angiogenesis by *miR-126* knockdown in vitro. In this regard, the Erk pathway inhibitor Spred1 (Taniguchi et al., 2007) was directly repressed by *miR-126* co-transfection and was upregulated in *miR-126* knockdown HUVEC (see Fig. S3 in the supplementary material).

Overall, the current studies describe essential in vivo regulation of angiogenesis by a miRNA as evidenced by delayed developmental vascularization in retina and brain, impaired adult VEGF-dependent corneal angiogenesis, and in vitro regulation of motility. Edema was a prominent feature of *miR-126*$^{\Delta/\Delta}$ embryos and was tightly correlated with the lethality observed in ~50% of embryos. This edema did not appear secondary to intrinsic cardiac defects (data not shown). The incompletely penetrant embryonic lethality and angiogenic delay of *miR-126*$^{\Delta/\Delta}$ mice contrast with the more classical embryonic lethal angiogenic phenotypes (Gale and Yancopoulos, 1999) and appear consonant with the comparatively subtle action of miRNAs in fine-tuning global gene expression profiles (Kloosterman and Plasterk, 2006; Zhao and Srivastava, 2007).

Consistent with its vascular expression pattern, these *miR-126* phenotypes occur cell-autonomously in endothelium as judged from the compartment-specific deletion phenotypes of *miR-126*$^{flox//\Delta}$*;Tie2-Cre* embryos. Mechanistically, this cell-autonomous action allows *miR-126* deficiency to derepress and overexpress the p85β regulatory subunit of PI3K and Spred1, which represent negative regulators of PI3K and MAP kinase signaling, respectively (see Fig. S4 in the supplementary material). Although p85β and Spred1 dysregulation clearly appears contributory to the *miR-126* phenotype, the promiscuous action of miRNA suggests the likely action of numerous additional target genes.

During the preparation of this manuscript, *miR-126* deletion phenotypes in mouse and knockdown in zebrafish were described with impaired angiogenesis and vascular integrity via dysregulation

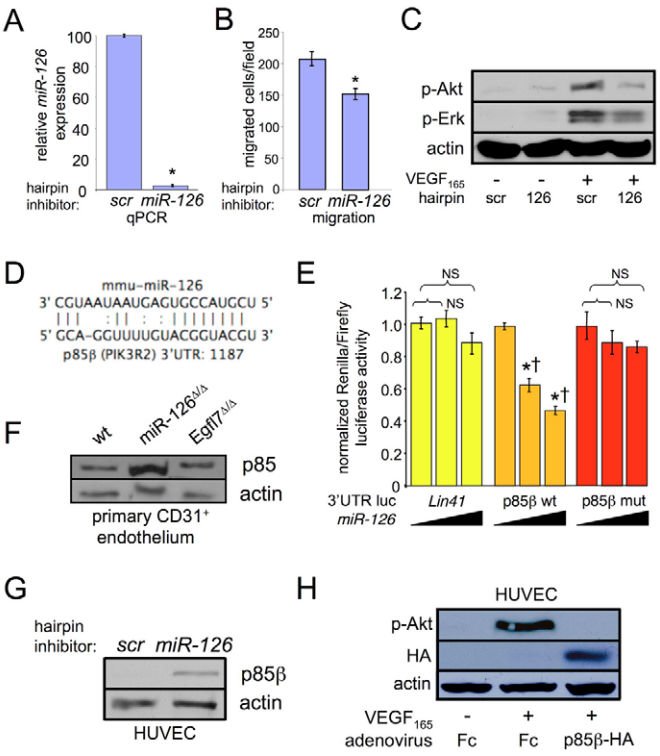

Fig. 4. Regulation of p85β expression by *miR-126*. (**A**) Quantitative PCR analysis confirms the almost complete absence of *miR-126* expression in HUVEC transfected with a *miR-126* hairpin inhibitor, as opposed to a scrambled control (scr). (**B**) Impaired migration of HUVEC transfected with the *miR-126* hairpin inhibitor, versus scr, in the in vitro scratch wound assay (*P<0.05 versus scrambled inhibitor-transfected). (**C**) Impaired VEGF-dependent Akt and Erk phosphorylation in HUVEC transfected with the *miR-126* hairpin inhibitor, versus scr. (**D**) Target site alignment for *miR-126* in the 3′UTR of *Pik3r2*, which encodes p85β. (**E**) p85β (*Pik3r2*) is a direct target *of miR-126* as shown by dose-dependent repression by *miR-126* of luciferase expression from the wild-type p85β 3′UTR, but not the control *Lin41* 3′UTR, reporters in 293T cells. Mutation of the *miR-126* binding site in the p85β 3′UTR (p85β mut) abrogates repression by *miR-126*, identifying p85β as a direct target. *P<0.05 versus no *miR-126* expression vector and †P<0.05 versus p85β mut and *Lin41* 3′UTR reporter construct, for a given dose of *miR-126* expression vector (0, 10 and 100 ng). NS, not significant. (**F**) p85 is upregulated in primary brain endothelial cells isolated from *miR-126*$^{\Delta/\Delta}$, but not *Egfl7*$^{\Delta/\Delta}$, mice as assessed by western blot with anti-pan p85 antibody; anti-actin antibody provided a loading control. (**G**) Upregulation of p85β expression in HUVEC transfected with a hairpin inhibitor targeting *miR-126*, versus scr. (**H**) Adenoviral expression of p85β in HUVEC is sufficient to inhibit VEGF-induced Akt phosphorylation.

of Spred1 and p85β (Fish et al., 2008; Wang et al., 2008). These phenotypes are both reinforced by similar findings in the current report and are extended by our analysis of endothelial-specific deletion in *miR-126*$^{flox//\Delta}$*;Tie2-Cre* embryos. Furthermore, an added significant feature of the current study is the unexpected lack of abnormalities in *Egfl7*$^{\Delta/\Delta}$ mice and the widespread phenocopying by *miR-126*$^{\Delta/\Delta}$ mice of vascular deficits of previously described *Egfl7* alleles, consisting of a gene-trap in intron 2 and a *lacZ* insertion into exons 5-7, both upstream of intron 7 that contains *miR-126* (Schmidt et al., 2007). These data indicate that *miR-126* might well regulate the collective migration of endothelium as has been proposed for

Egfl7 (Schmidt et al., 2007). These *miR-126*$^{\Delta/\Delta}$ mice should facilitate additional exploration of *miR-126* function in settings of adult angiogenesis, as well as of divergent *miR-126* roles such as in metastasis suppression (Tavazoie et al., 2008). Conversely, the *Egfl7*$^{\Delta/\Delta}$ mice will allow selective in vivo analysis of Egfl7 without the confounding influence of *miR-126*. Our data by no means exclude novel and essential *Egfl7*-specific functions, either alone or in conjunction with the paralog *Egfl8*, or as described in zebrafish knockdown, mouse overexpression and in vitro studies (Campagnolo et al., 2005; Lelievre et al., 2008; Soncin et al., 2003; Xu et al., 2008).

The inadvertent disruption of miRNA expression by conventional deletion and gene-trap knockout approaches in mice was recently predicted in a bioinformatics analysis by McManus and colleagues (Osokine et al., 2008). Our results comparing *miR-126*$^{\Delta/\Delta}$ and *Egfl7*$^{\Delta/\Delta}$ mice provide the most extensive documentation of this complication to date, which might be more widespread than anticipated; this possibility was not formally examined in the mouse *miR-126* deletion, as a parallel *Egfl7* knockout was not engineered (Wang et al., 2008). From these studies, evaluation of intronic miRNA should be a general consideration in the design and interpretation of mouse knockout studies (Osokine et al., 2008), and complications thereof might be avoided by utilizing minimally disruptive strategies such as floxed alleles covering small genomic regions. Finally, the regulation of angiogenesis by a mammalian miRNA suggests novel methods for the therapeutic modulation of vascularization, for instance during cancer or macular degeneration.

We are indebted to Gerald Crabtree, Andrew Fire, Cecile Chartier and Cullen Taniguchi for helpful discussions. *Hprt-Cre* mice and recombineering plasmids were kind gifts of Liqun Luo and Neal Copeland, respectively. This work was supported by grants from the NIH (1 R01 CA95654-01, 1 R01 NS052830-01 and 1 R01 HL074267-01) and the Brain Tumor Society to C.J.K.

Supplementary material

Supplementary material for this article is available at http://dev.biologists.org/cgi/content/full/135/24/3989/DC1

References

Barbour, L. A., Mizanoor Rahman, S., Gurevich, I., Leitner, J. W., Fischer, S. J., Roper, M. D., Knotts, T. A., Vo, Y., McCurdy, C. E., Yakar, S. et al. (2005). Increased P85alpha is a potent negative regulator of skeletal muscle insulin signaling and induces *in vivo* insulin resistance associated with growth hormone excess. *J. Biol. Chem.* **280**, 37489-37494.

Brachmann, S. M., Ueki, K., Engelman, J. A., Kahn, R. C. and Cantley, L. C. (2005). Phosphoinositide 3-kinase catalytic subunit deletion and regulatory subunit deletion have opposite effects on insulin sensitivity in mice. *Mol. Cell. Biol.* **25**, 1596-1607.

Campagnolo, L., Leahy, A., Chitnis, S., Koschnick, S., Fitch, M. J., Fallon, J. T., Loskutoff, D., Taubman, M. B. and Stuhlmann, H. (2005). EGFL7 is a chemoattractant for endothelial cells and is up-regulated in angiogenesis and arterial injury. *Am. J. Pathol.* **167**, 275-284.

De Maziere, A., Parker, L., Van Dijk, S., Ye, W. and Klumperman, J. (2008). Egfl7 knockdown causes defects in the extension and junctional arrangements of endothelial cells during zebrafish vasculogenesis. *Dev. Dyn.* **237**, 580-591.

Fish, J. E., Santoro, M. M., Morton, S. U., Yu, S., Yeh, R. F., Wythe, J. D., Ivey, K. N., Bruneau, B. G., Stainier, D. Y. and Srivastava, D. (2008). miR-126 regulates angiogenic signaling and vascular integrity. *Dev. Cell* **15**, 272-284.

Fitch, M. J., Campagnolo, L., Kuhnert, F. and Stuhlmann, H. (2004). Egfl7, a novel epidermal growth factor-domain gene expressed in endothelial cells. *Dev. Dyn.* **230**, 316-324.

Gale, N. W. and Yancopoulos, G. D. (1999). Growth factors acting via endothelial cell-specific receptor tyrosine kinases: VEGFs, angiopoietins, and ephrins in vascular development. *Genes Dev.* **13**, 1055-1066.

Gerber, H. P., McMurtrey, A., Kowalski, J., Yan, M., Keyt, B. A., Dixit, V. and Ferrara, N. (1998). Vascular endothelial growth factor regulates endothelial cell survival through the phosphatidylinositol 3′-kinase/Akt signal transduction pathway. Requirement for Flk-1/KDR activation. *J. Biol. Chem.* **273**, 30336-30343.

Kloosterman, W. P. and Plasterk, R. H. (2006). The diverse functions of microRNAs in animal development and disease. *Dev. Cell* **11**, 441-450.

Kloosterman, W. P., Wienholds, E., de Bruijn, E., Kauppinen, S. and Plasterk, R. H. (2006). In situ detection of miRNAs in animal embryos using LNA-modified oligonucleotide probes. *Nat. Methods* **3**, 27-29.

Kuehbacher, A., Urbich, C., Zeiher, A. M. and Dimmeler, S. (2007). Role of Dicer and Drosha for endothelial microRNA expression and angiogenesis. *Circ. Res.* **101**, 59-68.

Kuo, C. J., Farnebo, F., Yu, E. Y., Christofferson, R., Swearingen, R. A., Carter, R., von Recum, H. A., Yuan, J., Kamihara, J., Flynn, E. et al. (2001). Comparative evaluation of the antitumor activity of antiangiogenic proteins delivered by gene transfer. *Proc. Natl. Acad. Sci. USA* **98**, 4605-4610.

Lelievre, E., Hinek, A., Lupu, F., Buquet, C., Soncin, F. and Mattot, V. (2008). VE-statin/egfl7 regulates vascular elastogenesis by interacting with lysyl oxidases. *EMBO J.* **27**, 1658-1670.

Obernosterer, G., Martinez, J. and Alenius, M. (2007). Locked nucleic acid-based in situ detection of microRNAs in mouse tissue sections. *Nat. Protoc.* **2**, 1508-1514.

Osokine, I., Hsu, R., Loeb, G. B. and McManus, M. T. (2008). Unintentional miRNA ablation is a risk factor in gene knockout studies: a short report. *PLoS Genet* **4**, e34.

Parker, L. H., Schmidt, M., Jin, S. W., Gray, A. M., Beis, D., Pham, T., Frantz, G., Palmieri, S., Hillan, K., Stainier, D. Y. et al. (2004). The endothelial-cell-derived secreted factor Egfl7 regulates vascular tube formation. *Nature* **428**, 754-758.

Poliseno, L., Tuccoli, A., Mariani, L., Evangelista, M., Citti, L., Woods, K., Mercatanti, A., Hammond, S. and Rainaldi, G. (2006). MicroRNAs modulate the angiogenic properties of HUVECs. *Blood* **108**, 3068-3071.

Schmidt, M., Paes, K., De Maziere, A., Smyczek, T., Yang, S., Gray, A., French, D., Kasman, I., Klumperman, J., Rice, D. S. et al. (2007). EGFL7 regulates the collective migration of endothelial cells by restricting their spatial distribution. *Development* **134**, 2913-2923.

Soncin, F., Mattot, V., Lionneton, F., Spruyt, N., Lepretre, F., Begue, A. and Stehelin, D. (2003). VE-statin, an endothelial repressor of smooth muscle cell migration. *EMBO J.* **22**, 5700-5711.

Taniguchi, K., Kohno, R., Ayada, T., Kato, R., Ichiyama, K., Morisada, T., Oike, Y., Yonemitsu, Y., Maehara, Y. and Yoshimura, A. (2007). Spreds are essential for embryonic lymphangiogenesis by regulating vascular endothelial growth factor receptor 3 signaling. *Mol. Cell. Biol.* **27**, 4541-4550.

Tavazoie, S. F., Alarcon, C., Oskarsson, T., Padua, D., Wang, Q., Bos, P. D., Gerald, W. L. and Massague, J. (2008). Endogenous human microRNAs that suppress breast cancer metastasis. *Nature* **451**, 147-152.

Ueki, K., Fruman, D. A., Brachmann, S. M., Tseng, Y. H., Cantley, L. C. and Kahn, C. R. (2002). Molecular balance between the regulatory and catalytic subunits of phosphoinositide 3-kinase regulates cell signaling and survival. *Mol. Cell. Biol.* **22**, 965-977.

Wang, S., Aurora, A. B., Johnson, B. A., Qi, X., McAnally, J., Hill, J. A., Richardson, J. A., Bassel-Duby, R. and Olson, E. N. (2008). The endothelial-specific microRNA miR-126 governs vascular integrity and angiogenesis. *Dev. Cell* **15**, 261-271.

Xu, D., Perez, R. E., Ekekezie, II, Navarro, A. and Truog, W. E. (2008). Epidermal growth factor-like domain 7 protects endothelial cells from hyperoxia-induced cell death. *Am. J. Physiol. Lung Cell Mol. Physiol.* **294**, L17-L23.

Zhao, Y. and Srivastava, D. (2007). A developmental view of microRNA function. *Trends Biochem. Sci.* **32**, 189-197.